JOURNAL OF MATERIALS SCIENCE: MATERIALS IN MEDICINE **16** (2005) 699–707

Synthesis, characterization and melt spinning of a block copolymer of L-lactide and ε-caprolactone for potential use as an absorbable monofilament surgical suture

Y. BAIMARK, R. MOLLOY*, N. MOLLOY, J. SIRIPITAYANANON, W. PUNYODOM, M. SRIYAI
Biomedical Polymers Technology Unit, Department of Chemistry, Faculty of Science, Chiang Mai University, Chiang Mai 50200, Thailand
E-mail: robert@chiangmai.ac.th

This paper describes the synthesis and characterization of a block copolymer of L-lactide (LL) and ε-caprolactone (CL) and its subsequent melt spinning into a monofilament fiber. The synthesis reaction was a two-step process. In the first step, an approximately 50:50 mol% random copolymer, P(LL-*co*-CL), was synthesized via bulk copolymerization of LL and CL. This first-step prepolymer then became the macroinitiator in the second-step reaction in which more LL monomer was added to form a block copolymer, PLL-*b*-P(LL-*co*-CL)-*b*-PLL. Both the prepolymer and block copolymer were characterized by a combination of analytical techniques comprising dilute-solution viscometry, GPC, ^{1}H and ^{13}C NMR, DSC and TG. The block copolymer was then processed into a monofilament fiber using a small-scale melt spinning apparatus. The fiber was spun with a minimum amount of chain orientation and crystallinity so that its semi-crystalline morphology could be constructed under more controlled conditions in subsequent off-line hot-drawing and annealing steps. In this way, the fiber's tensile properties and dimensional stability were developed, as indicated by the changes in its stress-strain curve. The final drawn and annealed fiber had a tensile strength ($>$400 MPa) approaching that of a commercial PDS II suture of similar size. It is considered that this type of block copolymer has the potential to be developed further as a lower-cost alternative to the current commercial monofilament surgical sutures.
© *2005 Springer Science + Business Media, Inc.*

1. Introduction

During the past 3 decades, research interest in copolymers of L-lactide (LL) and ε-caprolactone (CL) has increased steadily as their potential in a wide range of biomedical applications has been realized. These applications have so far included biodegradable controlled-release drug delivery systems [1, 2], monofilament surgical sutures [3–6] and absorbable nerve guides [7]. By varying the copolymer composition, monomer sequencing and molecular weight, the copolymer properties can be tailored to meet the specific requirements of each particular application.

These copolymers have been shown to be both biocompatible and biodegradable [3, 5, 7]. Biodegradation proceeds via simple hydrolysis (random chain scission) leading to progressively lower molecular weight fragments. In the case of LL-rich fragments, hydrolysis usually continues unabated until L-lactic acid is formed. However, CL-rich fragments tend to be taken up in the final stage by macrophages and giant cells and degraded within these cells by enzymes before eventually yielding ε-hydroxycaproic acid. Both L-lactic acid and ε-hydroxycaproic acid are either metabolizable or excretable from the human body without any adverse toxicological effects.

Previous studies of the synthesis of poly(L-lactide-*co*-ε-caprolactone), P(LL-*co*-CL), random copolymers revealed the sensitivity of copolymer microstructure and molecular weight to the copolymerization conditions used [8–11]. For example, Grijpma and coworkers [8, 9] studied the effects of temperature and time and demonstrated the increasing importance of transesterification reactions as both temperature and time increased. Microstructural characterization of P(LL-*co*-CL) random copolymers, both in terms of their monomer sequencing and average monomer block lengths, has been described by several workers using ^{13}C NMR as the main analytical technique [10, 12, 13].

*Author to whom all correspondence should be addressed.

Since the two monomer reactivity ratios are quite different [9, 13], r_1 (LL) $>r_2$ (CL), tapered copolymers with some blocky character tend to be formed. However, transesterification, depending on the extent to which it occurs, tends to randomize the monomer sequencing.

Most of this previous work has concentrated on random copolymers since they can be synthesized in a single-step reaction and their microstructural characterization is well documented in the literature [8–13]. However, random P(LL-*co*-CL) copolymers tend to be largely amorphous over a wide intermediate range of composition. Whereas this may not be a serious problem in applications such as drug delivery systems and nerve guides, where low crystallinity can be used to advantage, surgical sutures require appreciable crystallinity in order to give the fiber its necessary tensile and knot-pull strengths. Consequently, it has proved difficult to tailor random P(LL-*co*-CL) copolymers to give the required balance of mechanical properties necessary for monofilament suture applications.

This present paper now addresses this problem by redesigning the copolymer structure to give a segmented triblock copolymer combining hard crystallizable end blocks with a soft flexibilizing center block, as in PLL-*b*-P(LL-*co*-CL)-*b*-PLL. This triblock structure is similar to that of the commercial suture 'MONOCRYL' (Ethicon, Johnson & Johnson) [14, 15] except that the main monomer component is L-lactide (LL) instead of the much more expensive glycolide upon which most commercial sutures, including 'MONOCRYL', are based. While this has the attraction of offering a substantial reduction in cost, ways need to be found to compensate for the increase in chain stiffness, and therefore suture modulus, in changing from glycolide to L-lactide. If this can be achieved, it would open up the possibility of producing lower-cost alternatives to the current commercial monofilament sutures.

2. Experimental

2.1. Materials

L(−)-lactide monomer, hereafter referred to as simply L-lactide, was synthesized by well established procedures from L(+)-lactic acid (Fluka) and purified by repeated recrystallization from distilled ethyl acetate until a mol% purity (DSC) of at least 99.9% was obtained. ε-Caprolactone (Fluka) monomer was purified by fractional distillation over calcium hydride under reduced pressure and stored over molecular sieves in a refrigerator. The molecular structures of these two comonomers are shown in Fig. 1.

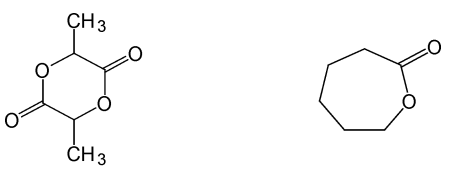

Figure 1 Molecular structures of the two comonomers: L(−)-lactide and ε-caprolactone.

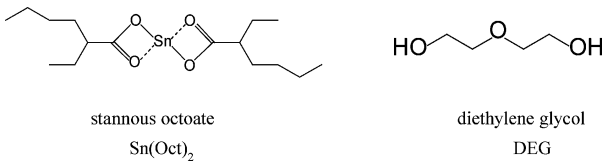

Figure 2 Molecular structures of the stannous octoate initiator and diethylene glycol coinitiator.

The stannous octoate (Sigma) initiator, $Sn(Oct)_2$, systematic name: tin(II) bis(2-ethylhexanoate), and the diethylene glycol (Fluka) coinitiator, DEG, were also purified by fractional distillation under reduced pressure and stored over molecular sieves at room temperature. Their molecular structures are shown in Fig. 2.

Ethyl acetate and toluene solvents, used for recrystallizing L-lactide and dissolving $Sn(Oct)_2$ respectively, were each purified by fractional distillation at normal pressure and stored over molecular sieves.

2.2. Copolymer synthesis

The synthesis of the block copolymer was a two-step reaction, as shown in Scheme 1. Prior to copolymerization, scrupulous attention was paid to the purities of the reagents and the dryness of the apparatus. Even trace

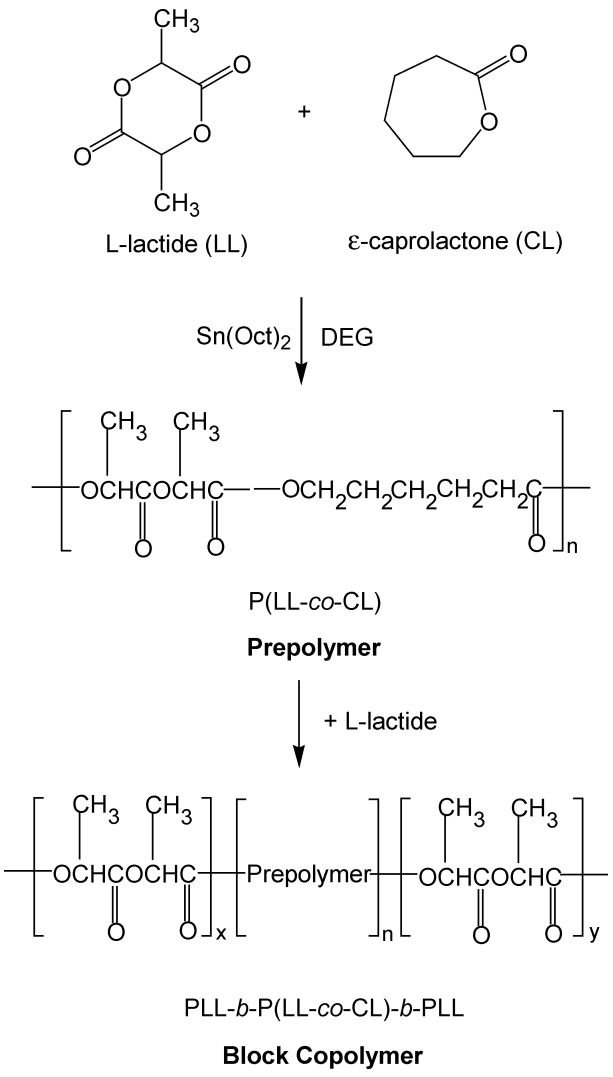

Scheme 1 Two-step preparation of the block copolymer.

amounts of moisture and/or other hydroxyl-containing impurities (e.g., L-lactic acid and ε-hydroxycaproic acid impurities in the monomers) can influence the molecular weight of the product. The chosen initiator-coinitiator combination was $Sn(Oct)_2$-DEG which is a common initiating system used in cyclic ester polymerization.

In the first-step reaction, L-lactide (LL) and ε-caprolactone (CL), in a LL:CL = 50:50 mol% ratio, were copolymerized in bulk at 140 °C for 48 h with stirring under a dry nitrogen atmosphere. The $Sn(Oct)_2$ and DEG concentrations relative to the total comonomer concentration were $[Sn(Oct)_2] = 0.005$ mol% and [DEG] = 0.21 mol%. For convenience and accuracy in weighing, $Sn(Oct)_2$ was prepared as a 0.8 M solution in dry toluene. At the end of the reaction, the random copolymer product, P(LL-*co*-CL), was allowed to cool, cut up into small pieces and dried to constant weight in a vacuum oven at 55 °C.

In the second-step reaction, the P(LL-*co*-CL) product from the first-step, hereafter referred to as the "prepolymer", was mixed with more LL monomer to give an overall LL:CL = 80:20 mol% ratio. The mixture was heated initially at 170 °C for 1.5 h to ensure complete melting and homogeneous mixing before the temperature was decreased to 160 °C for a further 12 h. Acting as a macroinitiator, the prepolymer polymerized the added LL monomer to give a triblock copolymer, PLL-*b*-P(LL-*co*-CL)-*b*-PLL, hereafter referred to as the "block copolymer", as shown in Scheme 1. At the end of the reaction, the final block copolymer product was cut up into small pieces and dried to constant weight in a vacuum oven at 100 °C.

2.3. Copolymer characterization

The intrinsic viscosity, $[\eta]$, of each copolymer was determined from flow-time measurements on a dilution series of solutions in chloroform as solvent at 30 °C using a Schott-Geräte AVS300 Automatic Viscosity Measuring System. The number-average molecular weight, $\bar{M}_n$, and polydispersity, PD, were determined by gel permeation chromatography (GPC) using a Waters 717 GPC equipped with an autosampler and Ultrastyragel® columns operating at 40 °C and employing universal calibration. Tetrahydrofuran (THF) was used as the solvent at a flow rate of 1 ml/min.

Copolymer composition and monomer sequencing were characterized by a combination of high-resolution 300 MHz ^{1}H and 75 MHz ^{13}C nuclear magnetic resonance (NMR) spectrometry using a Bruker Avance DPX 300 ^{1}H/^{13}C NMR Spectrometer. Spectra were obtained from copolymer solutions in deuterated chloroform ($CDCl_3$) at room temperature.

Thermal analysis was carried out by means of differential scanning calorimetry (DSC), using a Mettler Toledo DSC822, and thermogravimetry (TG) using a Perkin-Elmer TGA7 Thermogravimetric Analyzer. For DSC, copolymer samples of 5–10 mg in weight were heated at 10 °C/min under a nitrogen atmosphere over the temperature range −70 to 200 °C in order to observe their glass transition, T_g, crystallization, T_c, and crystalline melting, T_m, temperatures. For TG analysis, block copolymer samples of 5–10 mg in weight were heated at 20 °C/min under a nitrogen atmosphere over the temperature range 50 to 500 °C in order to assess their thermal stability for melt processing.

2.4. Fiber processing and testing

The melt spinning apparatus used for the block copolymer was a modular-design, small-scale fiber extruder manufactured by Ventures & Consultancy Bradford Ltd. (formerly Bradford University Research Ltd.), Bradford, UK. Its schematic arrangement is shown in Fig. 3 with a more detailed diagram of the compression, melting and metering zones, comprising the cylinder, heating block, filter mesh and spinnerette, shown in Fig. 4. The minimal dead volume within the system enabled sample sizes of as small as 10 g to be processed satisfactorily. To minimize void formation in the as-spun fibers, samples for melt spinning were best prepared as pre-formed rods. The water cooling bath was maintained at a temperature of 30 °C, while the vertical distance (air gap) between the spinnerette (single hole, 1 mm diameter) and the surface of the bath liquid was kept constant at 2 cm. Subsequent hot-drawing and annealing operations were performed off-line using a separate hot-drawing unit and vacuum oven respectively.

Following each stage of their production, the block copolymer monofilament fibers were characterized in terms of their uniformity of diameter and tested

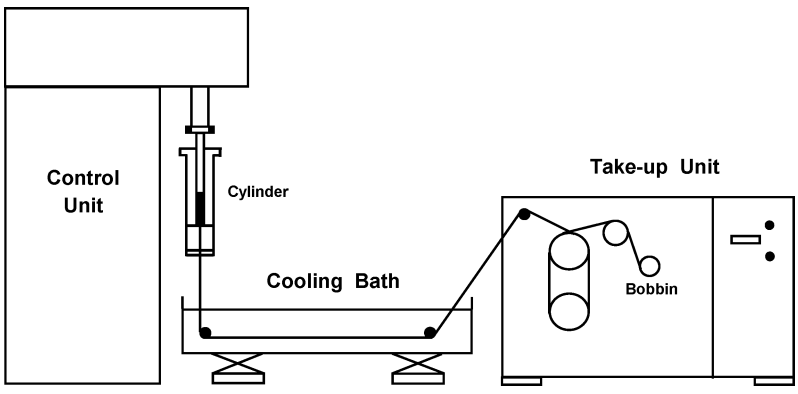

Figure 3 Schematic arrangement of the melt spinning apparatus.

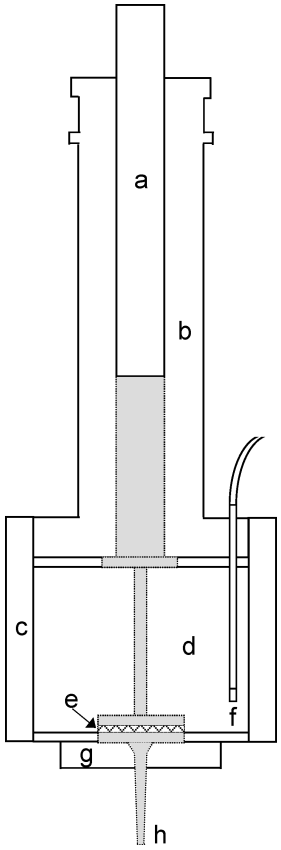

Figure 4 Schematic diagram of the compression, melting and metering zones showing the (a) ram, (b) cylinder, (c) band heater, (d) heating block, (e) stainless steel filter mesh, (f) thermocouple, (g) spinnerette, and (h) extruded monofilament fiber.

according to their solid-state morphology (DSC) and mechanical properties. Mechanical (tensile) testing was performed using a Lloyds LRX+ Universal Testing Machine equipped with bollard-type grips and a 100 N load cell.

3. Results and discussion

3.1. Copolymer synthesis

Both the prepolymer and the block copolymer were obtained in near-quantitative yield. This was concluded from the fact that, in each case, the weight loss due to residual monomer and/or low molecular weight oligomers on vacuum drying to constant weight was less than 5%.

Although this was not a mechanistic study, it is relevant to note here that ring-opening polymerization of cyclic esters using a $Sn(Oct)_2$-alcohol (ROH) combination as the initiating system is now widely accepted as occurring via a coordination-insertion type mechanism. However, the exact nature of the true initiating species has been the subject of much debate in the literature in recent years. Only recently, as reported for example by Kowalski and co-workers [16–18], has it been established that the true initiator is in fact the monoalkoxide, (Oct)Sn(OR), and/or the dialkoxide, $Sn(OR)_2$, generated *in situ* via the reaction between the $Sn(Oct)_2$ and the ROH. This debate and its conclusions have recently been reviewed by Albertsson and Varma [19].

TABLE I Molecular weight characteristics of the prepolymer and block copolymer

Polymer	$[\eta]$ [a] (dl/g)	$\bar{M}_n$ [b]	PD [c]
Prepolymer	1.00	5.4×10^4	1.74
Block Copolymer	1.26	7.4×10^4	1.88

[a]Intrinsic viscosity, as measured in chloroform as solvent at 30 °C.
[b]$\bar{M}_n$ = number-average molecular weight from GPC.
[c]PD = polydispersity from GPC = $\bar{M}_w/\bar{M}_n$.

3.2. Copolymer characterization

3.2.1. Molecular weight

Molecular weight characterization was carried out by means of a combination of dilute-solution viscometry and gel permeation chromatography (GPC). As confirmed in Table I, both the intrinsic viscosity, $[\eta]$, and number-average molecular weight, $\bar{M}_n$, values increased in going from the prepolymer to the block copolymer, consistent with chain extension. It is also significant to note that both copolymers gave unimodal molecular weight distributions, as shown by their GPC curves in Fig. 5, with the block copolymer exhibiting a slightly wider distribution and, hence, a slightly higher polydispersity (PD) value in Table I. The unimodal distribution of the block copolymer is particularly significant since it lends further support to the view that the final product is indeed a block copolymer rather than a polymer blend.

3.2.2. Composition and microstructure

Copolymer compositions were determined from the ^1H NMR spectra in Fig. 6 by ratioing the peak areas corresponding to the LL methine protons at $\delta = 5.0 - 5.3$ ppm and the CL ε-methylene protons at $\delta = 4.0 - 4.2$ ppm. The calculated compositions (LL:CL mol%) in Table II are seen to be within 2% of the corresponding comonomer ratios, as would be expected since the copolymerizations proceeded to near-quantitative conversion.

Monomer sequencing in the copolymers was characterized from the ^{13}C NMR spectra, specifically from the expanded carbonyl carbon (C=O) region from $\delta =$ 169–174 ppm, as shown in Fig. 7. The various peaks can be assigned to the C=O carbons of the middle units of various triad sequences, as labelled in Fig. 7. For example, the LCL peak appearing at about 172.8 ppm

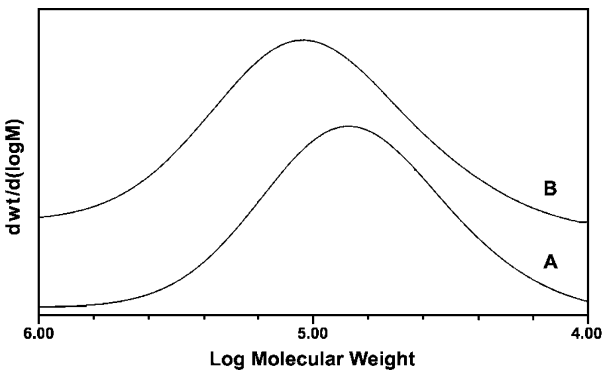

Figure 5 GPC curves of the prepolymer (A) and block copolymer (B).

TABLE II Chemical compositions and average monomer sequence lengths ($\bar{L}$) of the prepolymer and block copolymer

Polymer	Comonomer composition [a] LL:CL (mol%)	Copolymer composition [b] LL:CL (mol%)	$\bar{L}^c_{LL}$	$\bar{L}^c_C$
Prepolymer	50:50	52:48	3.1	2.3
Block copolymer	80:20	79:21	8.2	2.3

[a]Based on ratio of added monomers.
[b]As determined from the ^{1}H NMR spectrum.
[c]As determined from the expanded C═O region of the ^{13}C NMR spectrum.

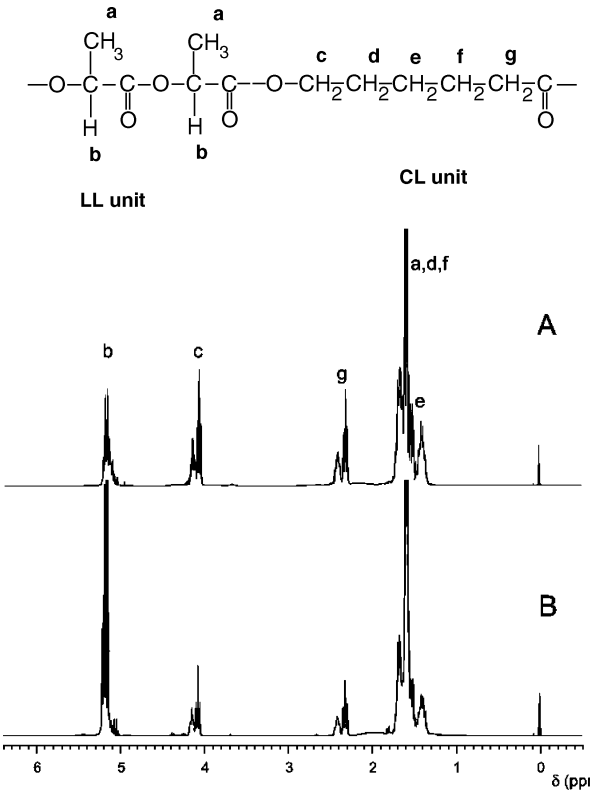

Figure 6 300 MHz ^{1}H NMR spectra of the prepolymer (A) and block copolymer (B) recorded in $CDCl_3$ as solvent at room temperature. (Peak-proton assignments as shown).

corresponds to the triad

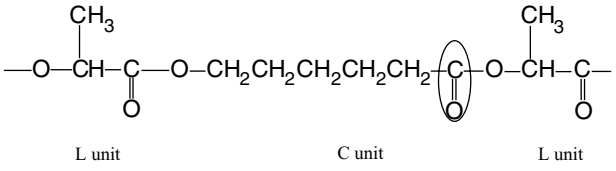

(NOTE: It should be explained here that, whereas LL and CL are the common abbreviations for the L-lactide and ε-caprolactone monomer units in the copolymer's structural formula, the abbreviations commonly used for designating triad sequences are simply L and C. In these designations, L refers to only a half-lactide unit, ─O─CH(CH_3)─CO─, in order to take account of their occurrence due to the cleavage of monomeric lactide units by transesterification.)

A more quantitative approach is possible through the use of Equations 1 and 2 which allow for calculation of the average monomer block lengths, $\bar{L}_{LL}$ and $\bar{L}_C$, of the respective monomer units from the triad peak

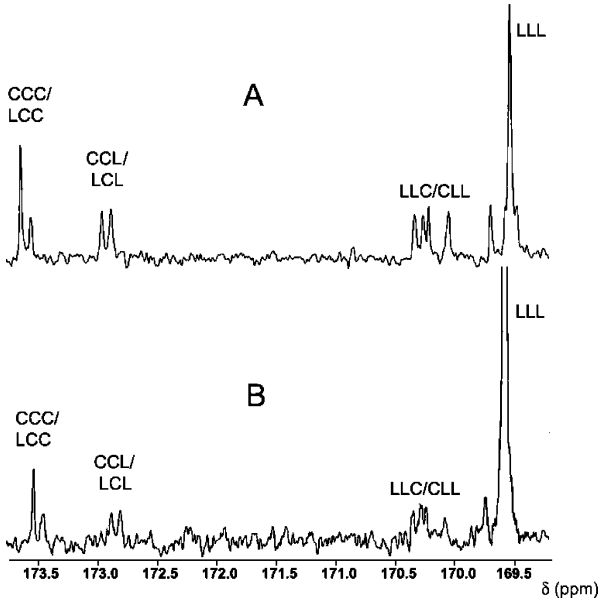

Figure 7 Expanded carbonyl regions of the 75 MHz ^{13}C NMR spectra of the prepolymer (A) and block copolymer (B) recorded in $CDCl_3$ as solvent at room temperature. (Peak-triad assignments as shown).

intensities (I) [13]. The various triad peaks which are referred to in these two equations are labelled in Fig. 7.

$$\bar{L}_{LL} = \frac{1}{2}\left[\frac{I_{LLL} + (I_{LLC} + I_{CLL})/2}{(I_{LLC} + I_{CLL})/2 + I_{CLC}} + 1\right] \quad (1)$$

$$\bar{L}_C = \frac{I_{CCC} + I_{LCC}}{I_{CCL} + I_{LCL}} + 1 \quad (2)$$

The $\bar{L}_{LL}$ and $\bar{L}_C$ values for the copolymers are given in Table II. For the prepolymer, of 52:48 mol% composition, values of 3.1 and 2.3 respectively are consistent with a slightly tapered rather than a purely random monomer sequencing. This is a consequence of the differing LL and CL monomer reactivity ratios. It should also be borne in mind that these $\bar{L}_{LL}$ and $\bar{L}_C$ values are underestimates of the "initial" values since they will have been decreased to some extent during the course of the copolymerization by the randomizing effect of transesterification. For the block copolymer, the $\bar{L}_C$ value of 2.3 reflects that of the prepolymer, as would be expected since the prepolymer forms the center block. The $\bar{L}_{LL}$ value, on the other hand, increases markedly up to 8.2 with the addition of the PLL end-blocks.

3.2.3. Temperature transitions

Thermal analysis of the copolymers was carried out by means of differential scanning calorimetry (DSC). Two successive heating scans were performed from −70 to 200 °C: the first on the copolymers as prepared (after storage) and the second immediately afterwards following cooling back to −70 °C. As shown in Fig. 8(A), the first scan of the prepolymer exhibits a clear, well defined glass transition over the range of −40 to −10 °C, with a mid-point $T_g = -21$ °C, but a very broad melting transition from 40–110 °C. The fact that the prepolymer can crystallize at all, despite its near equimolar composition, is a further indication that its monomer sequencing is tapered rather than random. However, after cooling

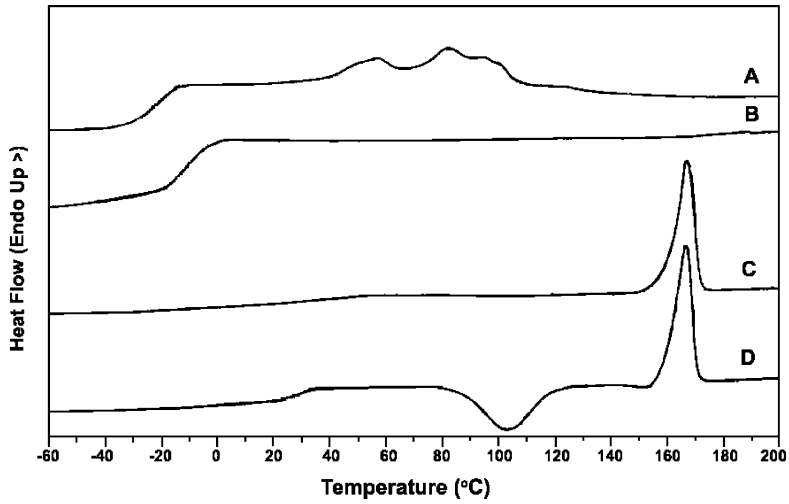

Figure 8 DSC thermograms (heating rate = 10 °C/min): first and second heating scans for the prepolymer (A, B) and block copolymer (C, D).

from the melt, the second scan in Fig. 8(B) shows only the glass transition with a $T_g = -10\,^{\circ}C$. Clearly, the prepolymer is unable to crystallize within the short timescale of the second scan. In order to crystallize, it requires prolonged storage at room temperature, which is effectively an annealing condition. The crystallizability on storage at room temperature of P(LL-*co*-CL) 50:50 random copolymers has also been reported by Tsuji and co-workers [20].

It is interesting to compare these prepolymer T_g values with that which can be calculated from the Fox Equation 3 for a random copolymer of known composition:

$$\frac{w_{LL}}{T_{g_{LL}}} + \frac{w_{CL}}{T_{g_{CL}}} = \frac{1}{T_{g_{LL-CL}}} \tag{3}$$

where w_{LL} and w_{CL} are the respective weight fractions of the LL and CL monomer units in the copolymer while $T_{g_{LL}}$ and $T_{g_{CL}}$ are the respective T_g (K) values of the PLL and PCL homopolymers. For a 52:48 mol% LL:CL prepolymer composition (Table II), $w_{LL} = 0.58$ and $w_{CL} = 0.42$. Substituting these and the reference T_g values [21] of $T_{g_{LL}} = 65\,^{\circ}C$ (338 K) and $T_{g_{CL}} = -60\,^{\circ}C$ (213 K) into Equation 3 yields a predicted random copolymer $T_{g_{LL-CL}} = -2\,^{\circ}C$. Comparing this with the experimental values in Table III, the prepolymer $T_g = -10\,^{\circ}C$ in the amorphous state is in reasonably close agreement. However, in its semicrystalline state, the prepolymer $T_g = -21\,^{\circ}C$ is nearly 20 °C lower than the predicted value, considerably closer to the T_g of PCL than PLL. This suggests that, when the prepolymer crystallizes, the amorphous regions are proportionately richer in CL units than the crystalline domains.

In marked contrast to that of the prepolymer, the first DSC scan of the block copolymer in Fig. 8(C) shows a single sharp melting peak at 150–170 °C due to the PLL end-blocks. After cooling and re-heating, the block copolymer's second scan in Fig. 8(D) shows a glass transition, a crystallization exotherm and a melting peak. The appearance of a single T_g is particularly interesting. Usually, block copolymers exhibit more than one T_g, one for each type of block. In the case of the PLL-*b*-P(LL-*co*-CL)-*b*-PLL block copolymer synthesized here, the T_g of P(LL-*co*-CL) has already been seen for the prepolymer to be below 0 °C, while the T_g of PLL is about 65 °C. Thus, for the block copolymer to have only a single T_g of 29 °C, intermediate between these two values, is indicative of an amorphous phase in which there is no appreciable microdomain separation between the hard PLL end-blocks and the soft P(LL-*co*-CL) center blocks. Such separation would lead to separate T_gs. The values of the various transition temperatures and corresponding heats of transition for both the prepolymer and the block copolymer are compared in Table III.

TABLE III Thermal characteristics of the prepolymer and block copolymer

Polymer	T_g^a (°C)	T_c^b (°C)	ΔH_c^c (J/g)	T_m^d (°C)	ΔH_m^e (J/g)
Prepolymer					
First heating scan	−21	–	–	59, 85	1.9, 5.8
Second heating scan	−10	–	–	–	–
Block copolymer					
First heating scan	–	–	–	169	35.3
Second heating scan	29	105	29.9	168	35.3

[a]Glass transition temperature (mid-point).
[b]Crystallization temperature (peak).
[c]Heat of crystallization (∝ % crystallization).
[d]Crystalline melting temperature (peak).
[e]Heat of melting (∝ % crystallinity).

3.2.4. Thermal stability

Thermal stability is an important consideration where the melt processing of aliphatic polyesters is concerned. Where their melting and thermal decomposition ranges are in close proximity, as is often the case, the polyester will have only a narrow "processing window", i.e. a narrow temperature range within which it can be processed without accompanying thermal decomposition. Higher temperatures and longer times favour transesterification reactions which both lower and broaden the molecular weight distribution. More importantly, the low molecular weight

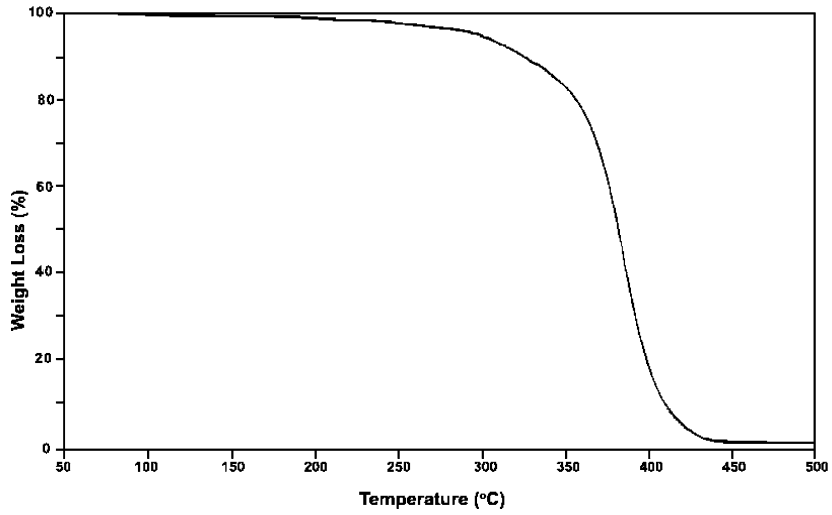

Figure 9 TG thermogram (heating rate = 20 °C/min) of the block copolymer.

thermal decomposition products which may be formed may be toxic to the human body in biomedical applications.

The choice of ε-caprolactone (CL) as the comonomer with L-lactide (LL) is partly related to this question of melt stability. Not only are CL units more flexible than LL units, they are also more thermally stable. Thus, copolymerization of CL with LL not only flexibilizes the copolymer, it also improves its melt stability. This is particularly relevant for producing surgical sutures where melt spinning is the preferred method of processing.

In this work, the thermal stability of the block copolymer was determined by thermogravimetry (TG). Its TG curve in Fig. 9 shows an initial decomposition (weight loss) temperature (T_d) of between 200–250 °C. When compared with the previous DSC curves in Figs. 8(C) and (D), which show that melting of the block copolymer is only complete at 180 °C, it tells us that the "processing window" is narrow but is at least positive. Based on this combined TG-DSC data, a melt spinning temperature of 190 °C was subsequently chosen, slightly above the melting range to lower the melt viscosity (improve the melt rheology) but still below T_d.

3.2.5. Fiber processing and testing

The block copolymer was melt spun into a monofilament fiber at a temperature of 190 °C through a single-hole spinnerette of diameter 1.0 mm. Employing just the minimum amount of on-line drawing necessary to maintain filament line stability, as-spun fibers of diameter 0.60 ± 0.02 mm were obtained. As confirmed by their DSC curve in Fig. 10(A) and stress-strain curve in Fig. 11, the as-spun fibers were largely amorphous and highly extensible due to their low degrees of chain orientation and crystallinity.

In order to transform these weak as-spun fibers into fibers with the necessary mechanical strength for suture applications, the required semi-crystalline morphology was built in under controlled conditions via separate off-line hot-drawing and annealing steps. After storing the as-spun fibers at room temperature for 5 days, they were hot-drawn in two separate stages at temperatures in between their glass transition and melting ranges. The conditions used were:

Stage 1 : hot-drawing at 60 °C to an off-line draw ratio of 4

Stage 2 : hot-drawing at 110 °C to an off-line draw ratio of 3

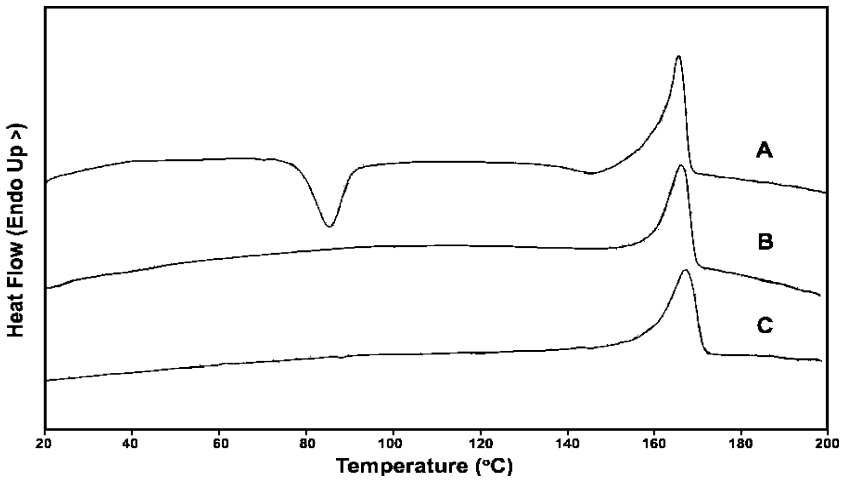

Figure 10 DSC thermograms (heating rate = 10 °C/min) of the as-spun (A), hot-drawn (B), and hot-drawn + annealed (C) block copolymer fibers.

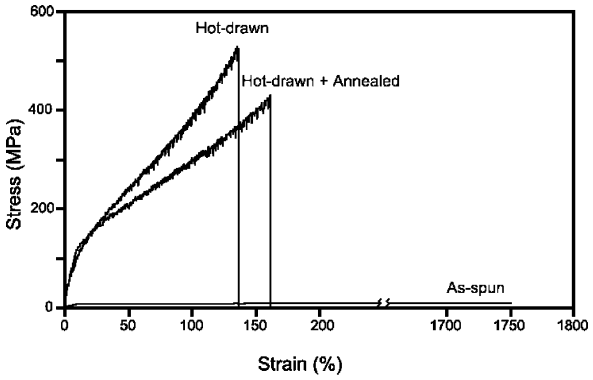

Figure 11 Stress-strain curves of the as-spun, hot-drawn and hot-drawn + annealed fibers of the block copolymer.

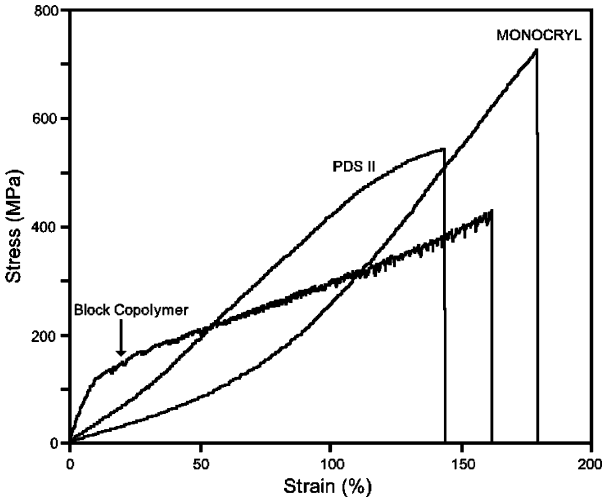

Figure 12 Comparison of the stress-strain curves of the block copolymer fiber (hot-drawn + annealed) with commercial 'PDS II' and 'MONOCRYL' size 4-0 monofilament sutures.

allowing equilibration back to room temperature in between. Thus, the total off-line draw ratio was $4 \times 3 = 12$. The hot-drawn fibers were then annealed at 80 °C for 5 h in a vacuum oven in order to allow molecular relaxation to take place within the fiber matrix. This improved the dimensional stability of the final fiber against shrinkage.

The final hot-drawn and annealed fibers had diameters of 0.16 ± 0.01 mm, similar in size to 'size 4-0' (0.15–0.20 mm) commercial sutures. The DSC curves in Figs. 10(B) and (C) and stress-strain curves in Fig. 11 clearly show how the hot-drawing operation introduces crystallinity and, hence, imparts mechanical strength to the fiber through orienting the copolymer chains along the fiber axis. Annealing, as previously mentioned, then serves mainly to facilitate molecular relaxation following the drastic changes in morphology brought about by hot-drawing. While this relaxation is thought to have relatively little effect on the crystalline orientation, it can bring about much more significant changes in the amorphous regions [22]. As seen in Fig. 11 and Table IV, the effect of annealing on the hot-drawn block copolymer fiber is to slightly decrease its stress at break (tensile strength) and initial modulus but slightly increase its elongation at break. The numerical values of these various properties are compared in Table IV.

Finally, the stress-strain curve of the block copolymer fiber is compared with those of the commercial sutures 'PDS II' and 'MONOCRYL' of similar size ('size 4-0') in Fig. 12, tested under identical conditions. The block copolymer is seen to have properties approaching those of 'PDS II', the main difference being its higher initial modulus. It is this property which determines the compliance and therefore the ease of handling of the fiber as a suture material.

TABLE IV Diameters and mechanical properties of the as-spun, hot-drawn and hot-drawn + annealed block copolymer fibers

Fiber	Diameter (mm)	Stress at break (MPa)	Elongation at break (%)	Young's modulus (initial) (MPa)
As-spun	0.60 ± 0.02	– [a]	– [a]	38
Hot-drawn	0.17 ± 0.01	529	135	1450
Hot-drawn + Annealed	0.16 ± 0.01	432	162	1224

[a]Fiber did not reach breaking point at limit of elongation (1750%).

4. Conclusions

The molecular architecture of the block copolymer, PLL-*b*-P(LL-*co*-CL)-*b*-PLL, described here was designed in such a way as to provide a balance between mechanical properties on the one hand and biodegradability on the other. In surgical terms, as far as a suture material is concerned, this translates as a balance between handling and healing properties. Although this paper has focussed its attention more on the mechanical than the biological side, it can be said that LL-CL copolymers have already been used successfully in biomedical applications (drug delivery systems and nerve guides) and been shown to be both biodegradable and biocompatible. What needs to be established for the block copolymer described here is the timescale for its biodegradation, both *in vitro* and *in vivo*, and its property loss-time profiles as a potential suture material. This will form the subject of a future paper.

One of the key elements in producing a new biomedical polymer, especially one that needs to biodegrade in the human body, is to be able to control its molecular architecture. In this work, this started with controlling the copolymer's chemical microstructure (composition, monomer sequencing) in the synthesis steps and finished with controlling the fiber's physical microstructure (matrix morphology, orientation) in the processing steps. Only by achieving this control can we expect to be able to produce a polymer which can meet the stringent property requirements of the application for which it is intended.

The combined analytical evidence presented here is consistent with the copolymer's purpose-designed segmented triblock structure. This, in turn, serves to support the synthesis methodology. Even so, more detailed studies of the synthesis conditions, including the choice of initiating system, could further enhance both molecular weight and microstructural homogeneity. These studies are currently in progress.

Following on from synthesis and characterization, fiber processing is a technology all of its own. Melt spinning is a complex multivariate process, as indeed are the temperature and time-dependent drawing and annealing steps. These various operations were purposely separated in order that (a) greater process control could be achieved and (b) the changes in matrix morphology with each step could be observed. In this way, it was possible to adjust and modify the fiber's oriented semicrystalline morphology and, at the same time, observe the effects on mechanical properties. X-ray diffraction (XRD) studies are also currently being carried out to confirm these changes.

In conclusion, the results presented here show that the block copolymer has the potential to be developed further as an absorbable monofilament suture. However, more "fine tuning" is still required in both synthesis and processing in order to increase the tensile strength and decrease the initial modulus (stiffness) of the final fiber. If this can be achieved, the block copolymer could provide a viable lower-cost alternative to the current commercial monofilament absorbable sutures. It is towards this end that work in the Biomedical Polymers Technology Unit in Chiang Mai is continuing.

Acknowledgments

The authors gratefully acknowledge Thailand's Development and Promotion of Science and Technology Talents (DPST) Program for providing a PhD scholarship for one of us (YB) and the National Metal and Materials Technology Center (MTEC) for its financial support for our Biomedical Polymers Technology Unit. We also wish to thank Dr. Sugunya Wongpornchai of the Department of Chemistry, Chiang Mai University, Chiang Mai, and Mrs. Patcharin Poochaiwatananoon of the Department of Chemistry, Mahidol University, Bangkok, for their help and advice with the NMR analyses.

References

1. A. SCHINDLER, R. JEFFCOAT, G. L. KIMMEL, C. G. PITT, M. E. WALL and R. ZWEIDINGERZ, in "Contemporary Topics in Polymer Science," edited by J. R. Pearce and E. M. Schaefger (Plenum, New York, USA, 1977) Vol. 2, p. 251.
2. H. GE, Y. HU, S. YANG, X. JIANG and C. YANG, *J. Appl. Polym. Sci.* **75** (2000) 874.
3. T. NAKAMURA, Y. SHIMIZU, T. MATSUI, N. OKUMURA, S. H. HYON and K. NISHIYA, in "Degradation Phenomena in Polymeric Materials," edited by H. Planck, M. Dauner and M. Renardy (Springer-Verlag, Berlin, Germany, 1992) p. 153.
4. J. P. PENNING, H. DIJKSTRA and A. J. PENNINGS, *Polymer* **34** (1993) 942.
5. K. TOMIHATA, M. SUZUKI, T. OKA and Y. IKADA, *Polym. Degrad. Stab.* **59** (1998) 13.
6. K. TOMIHATA, I SASAKI and M. SUZUKI, U.S. Patent No. 5,797,962 (1998).
7. W. F. A. DEN DUNNEN, B. VAN DER LEI, P. H. ROBINSON, A. HOLWERDA, A. J. PENNINGS and J. M. SCHAKENRAAD, *J. Biomed. Mater. Res.* **29** (1995) 757.
8. D. W. GRIJPMA, G. J. ZONDERVAN and A. J. PENNINGS, *Polym. Bull.* **25** (1991) 327.
9. D. W. GRIJPMA and A. J. PENNINGS, *ibid.* **25** (1991) 335.
10. E. J. CHOI, J. K. PARK and H. N. CHANG, *J. Polym. Sci., Part B: Polym. Phys. Edn.* **32** (1994) 2481.
11. M. HILJANEN-VAINIO, T. KARJALAINEN and J. SEPPÄLÄ, *J. Appl. Polym. Sci.* **59** (1996) 1281.
12. P. J. A. IN'T VELD, E. M. VELNER, P. VAN DE WITTE, J. HAMBUIS, P. J. DIJKSTRA and J. FEIJEN, *J. Polym. Sci., Part A: Polym. Chem. Edn.* **35** (1997) 219.
13. P. VANHOORNE, PH. DUBOIS, R. JEROME and PH. TEYSSIE, *Macromolecules* **25** (1992) 37.
14. R. S. BEZWADA, D. D. JAMIOLKOWSKI, I-Y. LEE, V. AGARWAL, J. PERSIVALE, S. TRENKA-BENTHIN, M. ERNETA, J. SURYADEVARA, A. YANG and S. LIU, *Biomaterials* **16** (1995) 1141.
15. R. S. BEZWADA, D. D. JAMIOLKOWSKI and S. W. SHALABY, U. S. Patent No. 5,133,739 (1992).
16. A. KOWALSKI, A. DUDA and S. PENCZEK, *Macromolecules* **33** (2000) 689.
17. A. KOWALSKI, J. LIBISZOWSKI, A. DUDA and S. PENCZEK, *ibid.* **33** (2000) 1964.
18. A. KOWALSKI, A. DUDA and S. PENCZEK, *ibid.* **33** (2000) 7359.
19. A-C. ALBERTSSON and I. K. VARMA, *Biomacromolecules* **4** (2003) 1466.
20. H. TSUJI, A. MIZUNO and Y. IKADA, *J. Appl. Polym. Sci.* **76** (2000) 947.
21. D. E. PERRIN and J. P. ENGLISH, in "Handbook of Biodegradable Polymers," edited by A. J. Domb, J. Kost and D. M. Wiseman (Harwood Academic Publishers, Amsterdam, Netherlands, 1997) Chapt. 1 and 3.
22. W. TANG, S. MURTHY, F. MARES, M. MCDONNELL and S. CURRAN, *J. Appl. Polym. Sci.* **74** (1999) 1858.

Received 30 June 2004
and accepted 17 December 2004